

CERN LIBRARIES, GENEVA



SCAN-9701128

IPNO-DRE-96-17

Transfer results for odd-odd ^{199}Au as a test of extended supersymmetry

*G. Berrier-Ronsin, G. Rotbard, M. Vergnes, S. Fortier,
J.M. Maison, L.-H. Rosier, and J. Verlotte*
Institut de Physique Nucléaire, 91406 Orsay Cedex, France

P. Van Isacker
GANIL, BP 5027, 14021 Caen Cedex, France

J. Jolie
Institut de Physique, Université de Fribourg,
Perolles, CH-1700 Fribourg, Suisse

SW9704

Transfer results for odd-odd ^{198}Au as a test of extended supersymmetry

G. Berrier-Ronsin, G. Rotbard, M. Vergnes, S. Fortier,
J. M. Maison, L-H. Rosier, and J. Vernotte
Institut de Physique Nucléaire, IN2P3-CNRS, F-91406 Orsay Cedex, France

P. Van Isacker
Grand Accélérateur National d'Ions Lourds, BP 5027, F-14021 Caen Cedex, France

J. Jolie
Institut de Physique, Université de Fribourg, Perolles, CH-1700 Fribourg, Suisse

Abstract

The nucleus ^{198}Au has been studied with an energy resolution of 11 keV via the $^{197}\text{Au}(d,p)^{198}\text{Au}$ reaction at an incident deuteron energy of 22 MeV. The angular distributions, measured at 10 angles, permit to clearly characterize the $l=1$ and 3 transfers. Data concerning the l values and spectroscopic strengths have been obtained; a comparison is made, for negative parity levels, between these results and theoretical energies, spins, and strengths calculated in the framework of extended supersymmetry. The results are also compared to those of a previous transfer study of ^{196}Au , and to another theoretical calculation.

PACS number(s): 21.10.Jx, 21.60.Fw, 25.45.Hi, 27.80.+w

I. INTRODUCTION

The formulation of the supersymmetry model of nuclear structure by Iachello [1] was motivated by the goal of unifying in a common framework, both even-even and odd-A nuclei. The common framework is a Lie superalgebra spanned both by Bose-like bilinear operators $b^\dagger b$ and $a^\dagger a$, and by Fermi-like bilinear operators $b^\dagger a$ and $a^\dagger b$ (for more details, see for example Chap. 4 of Ref. [2]). The same search for unification was responsible for the subsequent development [3,4] of an extended supersymmetric model to also include odd-odd nuclei.

Supersymmetry has been particularly successfully applied in the Pt region, ^{196}Pt being considered [5] as “the best O(6) nucleus.” The odd-A nuclei are described by the group $U_\pi(6/4)$ for odd Z and by the group $U_\nu(6/12)$ for odd N . In the extended supersymmetry, the group $U_\nu(6/12) \otimes U_\pi(6/4)$ describes a quartet of nuclei. Two such quartets expected [3,6–9] to be well described by this model, consist firstly of the nuclei ^{194}Pt , ^{195}Pt , ^{195}Au , and ^{196}Au , the odd-odd nucleus being ^{196}Au , and secondly of the nuclei ^{196}Pt , ^{197}Pt , ^{197}Au , and ^{198}Au , the odd-odd nucleus being ^{198}Au . Besides these two examples the model was also applied with success for the description of ^{194}Ir [10].

The odd-odd nucleus ^{196}Au has been studied experimentally via the $^{197}\text{Au}(p,d)^{196}\text{Au}$ reaction [6,7] and theoretically described in the above-mentioned framework. Although many new results have been obtained, the comparison with the model was obscured by the lack of sure knowledge concerning the J value for most of the ^{196}Au levels. Because the J values of low-lying levels in ^{198}Au are known [8,11] and because energies and spins of these levels have already been described with supersymmetry [9], it was hoped that the interpretation of transfer data in this case would be more meaningful.

The data presented and discussed in this paper have been obtained via the study of the neutron stripping $^{197}\text{Au}(d,p)^{198}\text{Au}$ reaction. The experimental procedures and methods of analysis, the data extracted concerning ^{198}Au , and the theoretical interpretation in the framework of the interacting boson and extended supersymmetry models, are described in the next sections.

II. EXPERIMENTAL PROCEDURE AND DWBA ANALYSIS

The (d,p) reaction has been studied using a 22 MeV deuteron beam from the Orsay MP tandem accelerator. The emitted protons were analyzed by the split-pole magnetic spectrometer and detected in the focal plane by a position- and angle-sensitive drift gas counter. Using a thin self-supporting gold target, the overall resolution was 11 keV (FWHM). A typical spectrum is shown in Fig. 1.

Angular distribution data were taken at 10 angles, between 5° and 50° . The absolute experimental cross sections $d\sigma/d\Omega$ were obtained from the determination of the target thickness ($95\mu\text{g}/\text{cm}^2$) through deuteron elastic scattering measurements. A local zero-range distorted-wave Born approximation (DWBA) analysis was performed with the code DWUCK4 [12], using the optical parameters of Table I (Refs. [13,14]), previously used to analyze the (p,d) reaction on Pt and Au isotopes (see [6] and Refs. therein). The spectroscopic factors $C^2 S_{l,j}$, and spectroscopic strengths $G_{l,j} = [(2J_f + 1)/(2J_i + 1)] C^2 S_{l,j}$ were obtained from comparison of the experimental and DWBA cross sections through the relation:

$$d\sigma(\theta)/d\Omega = N \sum_{l,j} G_{l,j} \sigma_{DW}^{lj}(\theta)/(2j+1) \quad (1)$$

[with $N=1.55$ as usually for the (d,p) reaction]. Contribution of both $l=1$ and $l=3$ angular momentum transfer may occur either for unresolved levels, or for any level with $J^\pi=1^-, 2^-$ or 3^- , since $|J_i - J_f| \leq j \leq J_i + J_f$, with $J_i=3/2$ for ^{197}Au .

As an example of the kind of agreement achieved, typical experimental angular distributions and the corresponding DWBA shapes are given in the upper part of Fig. 2 for two levels of ^{198}Au populated respectively by $l=1$ and $l=3$ angular momentum transfer. An example of angular distribution corresponding to a mixture is shown in the lower part. Since the observed cross section for a given spectroscopic strength is appreciably larger for a $l=1$ than for a $l=3$ transfer the determination of the strength for the $l=1$ part of the mixture is more precise than for the $l=3$ part.

III. EXPERIMENTAL RESULTS

It is apparent in Fig. 1, that most of the observed stripping cross-section lies at relatively low energy, below 600 keV. Above, peaks are observed but with weaker intensities up to 1.56 MeV and, after a large gap, several peaks with non-negligible strengths appear between 2.2 and 2.6 MeV.

Angular momentum l values have been assigned to most of the observed peaks and the corresponding spectroscopic strengths have been extracted. This extraction for $l=1$ and 3 was done with the assumption of $3p_{3/2}$ and $2f_{5/2}$ transfers. It has been checked that the DWUCK4 cross sections for the $j=l+1/2$ and the $j=l-1/2$ transfers are in a constant ratio, within less than 2% in the angular range in which the spectroscopic strengths are extracted. The ratio depends slightly on the excitation energy: between $Ex=0$ and 2.7 MeV, the ratio $G(j=l+1/2)/G(j=l-1/2)$ varies from 0.91 to 0.94 for $l=1$ and from 0.76 to 0.80 for $l=3$. The results up to 2.7 MeV are shown in Tables II, III and IV, together with already known data [8,11,15,16], in particular, excitation energies, spins, parities, and relative transfer cross sections. The uncertainties on the excitation energies due to the calibration are at most ± 4 keV up to 650 keV. They increase with excitation energy and could reach ± 8 keV.

Table II shows the experimental results for the lowest levels, below an excitation energy of 650 keV. In this energy domain, the few levels with a known positive-parity are weakly populated and could not be analyzed. Twenty seven negative-parity levels are known [11], but our experimental energy resolution of 11 keV allowed us to determine directly the spectroscopic strengths $G(l=1)$ and $G(l=3)$ only for fifteen peaks corresponding either to a single level or to a multiplet of known levels. To determine the distribution of strength among the members of a multiplet peak, we used the published results of a previous study [15,16] of the (d,p) reaction at 20 MeV on ^{197}Au , at only one angle (35°) but with a very good energy resolution (2.5 to 3.5 keV FWHM). It can be seen in Table II that the relative values of cross sections at 35° , measured at 22 MeV in the present work, are in good agreement for the whole energy domain considered with the ones of Ref. [15], although they disagree above ≈ 300 keV with the ones of Ref. [16]. It should be stressed however that the unexplained disagreement above 300 keV between Ref. [15] and Ref. [16] does not concern the ratio of cross sections for members of the multiplets unresolved in our work. This ratio can therefore

be used safely to evaluate the distribution of spectroscopic strength between the members of these multiplets. The result is shown in the last two columns of Table II. Such an evaluation is straightforward in the case of a single momentum transfer (peak at 543 keV for example) : the spectroscopic strength is then distributed proportionally to the cross sections at 35° . It is more complicated in the case of a mixture of transferred angular momentum. We have used the fact that, both at 20 and at 22 MeV and for the whole energy domain concerned, the cross sections at 35° are very similar for a pure $l=3, j=5/2$ transfer with $G=1$, and for a pure $l=1, j=3/2$ transfer with $G=0.3$. Accordingly, the quantity distributed proportionally to the cross section at 35° is in this case: $G(l=1)+0.3G(l=3)$. In the special case of the 343 keV peak, it is clear that all the $l=3$ strength can be attributed to the 346.7 keV level, because the 339.3 keV 0^- level can only be populated by a pure $l=1, j=3/2$ transfer. In the other cases limiting values are given.

Table III shows the results of the (d,p) reaction between 650 keV and 1.56 MeV.

The whole region between 1.56 and 2.7 MeV has been analyzed but the high density of levels often precludes an easy separation of the peaks. Moreover the angular distributions of some peaks are incomplete, due to the broad peaks corresponding to the (d,p) reaction on light impurities of the target. When possible, i.e. for strongly populated levels or groups of levels, data were extracted and are shown in Table IV. The maximum total strengths extracted in this whole region are: $G_1 = 0.16$; $G_3 = 2.67$.

IV. SUMMED SPECTROSCOPIC STRENGTHS

Before discussing the present stripping data, it is useful to first recall a few results obtained in our previous pick-up experiments. The total observed strengths, extracted from Table V of Ref. [6] and shown here in Table V are very similar (both for $l=1$ and for $l=3$) in the neutron pick-up reactions on ^{196}Pt and on ^{197}Au . This is consistent with similar occupation probabilities of the neutron orbitals concerned ($p_{1/2}$, $p_{3/2}$, $f_{5/2}$, and $f_{7/2}$) in these two target nuclei with $N=118$.

Going back now to the present neutron stripping experiment on ^{197}Au , it is interesting to look at the distribution of the different strengths ($l=1$ and 3) according, both to the excitation energy and to partial strengths of the individual fragments. We have, somewhat arbitrarily, taken (as in Ref. [6]) for the G values given in columns 4 and 5, an energy threshold at 600 keV and a strength threshold at $G=0.08$. The fragments with $G \geq 0.08$ will be called "large fragments". The ^{198}Au data concerning the summed strengths are summarized in the third column of Table VI. An important part of the strength is concentrated below 600 keV on a few large fragments (75% on 6 fragments for $l=1$ and 68% on 9 fragments for $l=3$, if we consider only the spectrum up to 1.56 MeV, 69% and 44% if we go up to 2.7 MeV).

It is also of interest to compare the summed strengths presently determined to the ones observed in previous studies of the neutron stripping on even-even targets, also with $N=118$. This, unfortunately, is possible only for the ^{196}Pt target, no precise result being available for the stripping on ^{198}Hg . To permit a meaningful comparison with our strengths (calculated in a local, zero range approximation), the Pt summed strengths extracted in Ref. [17] have been renormalized (multiplied by a factor 1.3) according both to the discussion in section 3.1 of Ref. [17], and to DWBA calculations. These renormalized Pt strengths are given in

the fourth column of Table VI and can be compared to the present Au strengths shown in the third column of the same table. The $l=1$ summed strengths for Au appear reasonably similar to the values found for Pt. However, the $l=3$ summed strength for Au below 600 keV is appreciably larger than the experimental value for Pt.

It is possible to go further. Indeed, looking in detail at the results of Ref. [17], it appears that only a small fraction (between 15 and 23%) of the $l=3$ strength observed below 600 keV in ^{197}Pt corresponds to a $j=7/2$ transfer. If we first assume the percentage to be the same in the present stripping experiment on ^{197}Au , we are left with a minimum summed strength for $j=5/2$ transfer of $G=2.6$ in ^{198}Au , about 1.3 times larger than the maximum one observed in the same energy domain in ^{197}Pt (2.1). If on the other hand we now assume the $j=5/2$ strength in ^{198}Au to be only the same (1.9) as the well-established $j=5/2$ strength in ^{197}Pt , then the $j=7/2$ strength in ^{198}Au below 600 keV is at least 2.8 times larger than in ^{197}Pt .

Since the occupation probabilities of the neutron orbits in the two target nuclei appear, as shown at the beginning of the present section, quite similar, we are led to conclude that a large part of the $l=3$ strength in the final nucleus (perhaps both for $j=5/2$ and for $j=7/2$) lies appreciably lower in energy in ^{198}Au than in ^{197}Pt , which in particular leads to the possibility of non negligible $j=7/2$ components in many ^{198}Au levels below 600 keV. This unexpected situation will be our main problem in the interpretation of the present experimental results.

The total $l=1$ and $l=3$ strengths extracted up to 2.7 MeV in the reaction $^{197}\text{Au}(d, p)^{198}\text{Au}$ are $G_1=2.0$ and $G_3=7.5$. The total measured strength $G_1 + G_3=9.5$ is consistent with the sum rule limit of 8, considering the uncertainty on absolute values of spectroscopic strengths ($\sim 20\%$) and the difference between extracted spectroscopic strengths for a $j=5/2$ transfer as assumed and for a $j=7/2$ as possible. It should finally be noted that the total summed strengths [$\sum C^2S + \sum G$] observed for both the pick-up and the stripping reactions on the $N=118$ target nuclei ^{197}Au (5.3 for $l=1$ and 13.7 for $l=3$) and ^{196}Pt (5.2 for $l=1$ and 11.3 for $l=3$) are in reasonable agreement with the sum rule limits (6 for $l=1$ and 14 for $l=3$).

V. THEORETICAL INTERPRETATION OF THE ^{198}AU RESULTS

Many models have been used to describe nuclei in the Pt-Au-Hg transition region. Most of these calculations give the level scheme and sometimes the electromagnetic properties, while a few give the transfer properties. This is especially true when the final nucleus is odd-odd. In this section our transfer results for the stripping reaction leading to ^{198}Au will be compared to two different calculations: an analytic supersymmetry calculation and a numerical interacting boson-fermion-fermion (IBFFM) calculation. Both consider an $O(6)$ boson core and simply ignore the $f_{7/2}$ neutron shell (the first by construction and the second because of numerical constraints).

A. Supersymmetry calculation

As for our earlier work on the odd-odd nucleus ^{196}Au [6] the theoretical interpretation of the experimental results can be carried out in the context of the $U_\nu(6/12) \otimes U_\pi(6/4)$ symmetry scheme [3]. Referring for more details on the formalism of this model to chapters 8

and 9 of [2] and for an application of it to [6], we repeat here only some of the limitations and assumptions at the basis of this approach. Only the negative-parity levels of ^{198}Au are considered and these are thought to arise from the neutron $3p_{1/2}$, $3p_{3/2}$, and $2f_{5/2}$ orbits and a proton $2d_{3/2}$ orbit. By assuming an $O(6)$ ^{196}Pt core as well as specific neutron-core, proton-core, and neutron-proton interactions, an analytic solution of the IBFFM Hamiltonian can be found. This allows the determination of energies and wave functions of the states in the odd-odd nucleus, from where other observables such as transfer reaction rates can be deduced. More specifically, a set of quantum numbers

$$|[N_1, N_2, N_3](\bar{\sigma}_1, \bar{\sigma}_2, \bar{\sigma}_3)(\sigma_1, \sigma_2, \sigma_3)(\tau_1, \tau_2)LJ| \quad (2)$$

can be assigned to each level with spin J in ^{198}Au which then has an energy

$$\begin{aligned} E(N_i, \bar{\sigma}_i, \sigma_i, \tau_i, L, J) = & A[N_1(N_1 + 5) + N_2(N_2 + 3) + N_3(N_3 + 1)] \\ & + \bar{B}[\bar{\sigma}_1(\bar{\sigma}_1 + 4) + \bar{\sigma}_2(\bar{\sigma}_2 + 2) + \bar{\sigma}_3^2] \\ & + B[\sigma_1(\sigma_1 + 4) + \sigma_2(\sigma_2 + 2) + \sigma_3^2] \\ & + C[\tau_1(\tau_1 + 3) + \tau_2(\tau_2 + 1)] \\ & + D L(L + 1) + E J(J + 1), \end{aligned} \quad (3)$$

where A , \bar{B} , B , C , D , and E are parameters which are fitted to the experimental energies of the excited states in the quartet of nuclei $^{196,197}\text{Pt}$ and $^{197,198}\text{Au}$.

The primary purpose of the present experimental study is to determine whether the assignments proposed on the basis of the energy fit are confirmed by the intensities in the $^{197}\text{Au}(d, p)^{198}\text{Au}$ neutron-transfer reaction. The transfer operators for this particular reaction are of the form

$$\hat{P}^{(j)} = \sum_{lj'} p_{lj'}^{(j)} [\bar{b}_l \times a_{j'}^\dagger]^{(j)}, \quad (4)$$

where $\bar{b}_{lm} = (-)^{l-m} b_{l-m}$ annihilates a neutron boson with angular momentum l , $a_{j'm'}^\dagger$ creates a neutron fermion in orbit j' , and $p_{lj'}^{(j)}$ are coefficients. The transferred angular momentum is j . One of the main difficulties in the application of (4) is the number of parameters $p_{lj'}^{(j)}$ in the transfer operator. In a previous study of this type [18] involving the even-even to odd-neutron reaction $^{196}\text{Pt}(d, p)^{197}\text{Pt}$, this number is reduced by considering transfer operators that have a definite tensor character under certain symmetry groups. Since our specific aim here is the study of quantum numbers associated to the levels, we do not wish to make additional assumptions about the transfer operator, that is, we wish to take the most general (lowest-order) operator as given in (4). Its form can be determined using $^{196}\text{Pt}(t, d)^{197}\text{Pt}$ data [17], normalized as indicated in section IV, together with the expression for the matrix elements of the different components in the transfer operator between the $O(6)$ even-even ground state and states in the odd-neutron nucleus:

$$\begin{aligned} & \langle [N_1, N_2](\sigma_1, \sigma_2, 0)(v_1, v_2)LJ \parallel [\bar{b}_l \times a_{j'}^\dagger]^{(j)} \parallel [N](N, 0, 0)(0, 0)0 \rangle \\ & = (-)^{j+1/2} \left[\frac{(2L+1)(2j+1)(2j'+1)}{2l+1} \right]^{1/2} \left\{ \begin{matrix} l & l' & L \\ \frac{1}{2} & j & j' \end{matrix} \right\} \delta_{Jj} \end{aligned}$$

$$\begin{aligned}
& \times \left\langle \begin{array}{cc} [N-1] & [1] \\ (N-1, 0, 0) & (1, 0, 0) \end{array} \middle| \begin{array}{c} [N_1, N_2] \\ (\sigma_1, \sigma_2, 0) \end{array} \right\rangle \\
& \times \left\langle \begin{array}{cc} (N-1, 0, 0) & (1, 0, 0) \\ (v, 0) & (v', 0) \end{array} \middle| \begin{array}{c} (\sigma_1, \sigma_2, 0) \\ (v_1, v_2) \end{array} \right\rangle \\
& \times \left\langle \begin{array}{cc} (v, 0) & (v', 0) \\ l & l' \end{array} \middle| \begin{array}{c} (v_1, v_2) \\ L \end{array} \right\rangle \\
& \times \langle [N](N, 0, 0)(0, 0)0 \parallel b_i^\dagger \parallel [N-1](N-1, 0, 0)(v, 0)l \rangle. \tag{5}
\end{aligned}$$

The symbol in curly brackets is a Racah coefficient and the three symbols in angle brackets are $U(6) \supset O(6)$, $O(6) \supset O(5)$, and $O(5) \supset O(3)$ isoscalar factors, respectively, which are listed in [2]. Note also that the boson operator in the reduced matrix element in (5) refers to a neutron boson and as a result this reduced matrix element equals the corresponding IBM-1 matrix element times $\sqrt{N_\nu/N}$.

The classification of levels used in ^{197}Pt is shown in Table VII, together with the spectroscopic strengths in the $^{196}\text{Pt}(t, d)^{197}\text{Pt}$ reaction. The first three columns give the measured spin-parity and energy, and the quantum numbers as they are assigned in [19]. The last two columns list the renormalized measured strengths from [17] and the ones calculated from (5). For several states no strength is observed in which case we have assumed zero (denoted by ~ 0). We note that more than 90% of the calculated strengths (both for $l=1$ and for $l=3$) is found below 600 keV in ^{197}Pt .

The data shown in Table VII allow the determination of all parameters in the transfer operator (4) and we find

$$\begin{aligned}
p_{0,1/2}^{(1/2)} &= 0.276, & p_{2,3/2}^{(1/2)} &= 0.340, & p_{2,5/2}^{(1/2)} &= 0.596, \\
p_{0,3/2}^{(3/2)} &= 0.187, & p_{2,1/2}^{(3/2)} &= -0.198, & p_{2,3/2}^{(3/2)} &= -0.006, & p_{2,5/2}^{(3/2)} &= 0.852, \\
p_{0,5/2}^{(5/2)} &= 0.347, & p_{2,1/2}^{(5/2)} &= -0.348, & p_{2,3/2}^{(5/2)} &= -0.124, & p_{2,5/2}^{(5/2)} &= 0.247.
\end{aligned} \tag{6}$$

In fact, because the equations are quadratic in $p_{l,j'}^{(j)}$, several solutions exist which give *exactly* identical results for the $^{196}\text{Pt}(t, d)^{197}\text{Pt}$ reaction. Since any of these solutions leads to approximately equivalent results for the $^{197}\text{Au}(d, p)^{198}\text{Au}$ reaction, we may limit ourselves to one of them.

The strengths for the $^{197}\text{Au}(d, p)^{198}\text{Au}$ reaction can now be calculated and are given in Table VIII, together with the currently measured values for the energy domain below 600 keV. The assignment of quantum numbers to the experimental levels is different from the one proposed in [9] in two respects:

- i) The 347 keV level, previously assigned $J^\pi = 1^-, 2^-$ on the basis of the average resonance capture technique [8], is now confirmed [11] to have spin $J^\pi = 2^-$ while the suggested spin in the calculation of [9] is $J^\pi = 1^-$. This necessitates some reassignments of $J^\pi = 1^-$ and $J^\pi = 2^-$ levels at higher energies. Note, however, that for all other levels below 450 keV with previously ambiguous spin, the assignment suggested in [9] is confirmed.
- ii) The quantum numbers of the lowest two $J^\pi = 3^-$ states are reversed. This reversal of the 3^- levels is suggested by the measured spectroscopic factors. The same inversion was proposed also earlier on the basis of a comparison between measured and calculated electromagnetic decay properties in ^{198}Au [20]. The reversal leads to a noticeably worse fit

as the root-mean-square deviation increases to 66 keV, compared to 51 keV in [9]. Although the root-mean-square deviation σ_{rms} is comparable to the level spacing in the odd-odd nucleus, it is not different from those obtained in supersymmetric description of the much simpler odd-A and even-even nuclei. For instance, the systematic study of Vervier [21] which includes seventeen cases gives an average value of $\sigma_{rms} = 89$ keV.

The resulting energy spectrum is shown in Fig. 3. It is obtained with parameters (in keV) $A + \bar{B} = 111$, $B = -101$, $C = 45$, $D = 47$, and $E = -30$. These parameters are close to those given in [9] (116, -100, 51, 52, and -32, respectively) and those (104, -99, 38, 42, and -23) obtained by comparing the theoretical and measured gamma branchings [20]. Note that only the sum $A + \bar{B}$ can be determined since all levels considered in the fit have $\bar{\sigma}_i = N_i$; as a result the labels $\bar{\sigma}_i$ have been dropped. It is encouraging that both the transfer amplitudes and the electromagnetic decay probabilities suggest the same assignment of quantum numbers. As a result similar parameter sets are found which are in turn close to those obtained from the other three members of the quartet. The similarity thus gives confidence in the extended supersymmetry approach.

The number of negative parity levels predicted below 600 keV, 28, is close to 25, the number of already known levels [11] in the same energy domain. The distribution of these predicted levels as a function of J (two $J=0$, eighth $J=1$, eighth $J=2$, seven $J=3$, and three $J=4$) is also in reasonable agreement with the observations [11]. As far as the stripping strengths are concerned, the model predicts that 85% of the total $l=3$ ($f_{5/2}$) strength, but only 68% of the $l=1$ ($p_{1/2}$ and $p_{3/2}$) should be observed below 600 keV.

For the total strengths in the energy domain below 600 keV, the agreement between the model and experiment is better for $l=1$ (1.26 and 1.49) than for $l=3$ (1.86 and 3.36). But as already stressed at the end of section IV, the disagreement for $l=3$ may be, at least partly, due to the existence for low energy levels in ^{198}Au , of sizeable $l=3$ ($f_{7/2}$) transfer components.

To allow an easier comparison level by level between experiment and theory, as well as a global overview, the data of Table VIII are displayed graphically in Fig. 4.

B. IBFFM calculation

The authors of Ref. [16] have performed an IBFFM calculation for ^{198}Au , assuming an $O(6)$ even-even core, and they have computed (among other quantities) the (d,p) spectroscopic factors $S_{l,j}$. The details and parameters of this calculation can be found in Ref. [16]. The spectroscopic strengths $G_{l,j} = [(2J_f + 1)/(2J_i + 1)]S_{l,j}$, calculated from Table 10 of Ref. [16], are also compared in Fig.4 to our data. Approximative values of the calculated energies have been extracted from Fig.4 of Ref. [16]. The individual results, level by level, are different from ours (Section V.A) but the overall agreement with experiment is not better. The summed strength below 600 keV equals 1.57 for $l=1$ and 1.63 for $l=3$. These values are similar to the ones obtained from the supersymmetric calculation. The fragmentation is, however, poorly reproduced compared to the supersymmetric calculation which agrees better with the experimental situation (see Fig.4).

VI. CONCLUSION

The present experimental data represent an improvement over what was previously known about ^{198}Au . It is now one of the few odd-odd nuclei for which detailed information is available concerning energy levels, electromagnetic transitions, and one-particle transfer amplitudes. The presently gathered information provides a good test of theoretical descriptions of this odd-odd nucleus.

So, what can be concluded from the present analysis, especially as regards the validity of the extended supersymmetry for odd-odd nuclei in this mass region? Although a reasonable overall description of ^{198}Au is obtained (with the notable exception of $l = 3$ strength), it must be admitted that the symmetry calculation has difficulties to account for the detailed structure of this nucleus. One of the main reasons is the unexpected observation of large $l=3$ transfer strength in this study. This strength which should be related to the $f_{7/2}$ orbit was not anticipated on the basis of prior studies in the odd-mass Pt isotopes and therefore the $f_{7/2}$ components are absent in the calculations. Besides this major discrepancy one should also consider the many complications that are to be expected as a result of the transitional nature of the collective excitations (intermediate between vibrational and rotational) and the interplay with single-particle features such as the core-particle or neutron-proton interactions. All these effects are present in the odd-odd nucleus ^{198}Au . Their supersymmetric description is only approximative and the compounded effect of the approximations leads to an overall deterioration in the agreement with the data.

It thus appears that extended supersymmetry, however elegant in its formulation, can give but a description of global properties of ^{198}Au (such as the level density) and even that only with certain limitations due to a restricted single-particle space. A detailed level-by-level description of the odd-odd nucleus is more difficult to obtain, but at present no other model seems available that can more adequately describe odd-odd nuclei in this transitional region.

There is, perhaps, room for some improvement in the supersymmetric description of odd-odd nuclei. As shown in [22] it is possible to decouple the concept of supersymmetry from that of dynamical symmetry and to propose a single hamiltonian for even-even and odd-mass nuclei which does not have a dynamical symmetry. This idea can be extended to odd-odd nuclei and involves the proposal of a single hamiltonian for quartets of nuclei but not restricted to a symmetry limit.

ACKNOWLEDGMENTS

This work is partly supported (JJ) by the Swiss National Science Foundation. PVI thanks the French Centre National de la Recherche Scientifique for a financial support.

REFERENCES

- [1] F. Iachello, *Phys. Rev. Lett.* **44**, 772 (1980).
- [2] F. Iachello and P. Van Isacker, *The Interacting Boson-Fermion Model*(Cambridge University Press, Cambridge, 1991).
- [3] P. Van Isacker, J. Jolie, K. Heyde, and A. Frank, *Phys. Rev. Lett.* **54**, 653 (1985).
- [4] A. B. Balentekin and V. Paar, *Phys. Rev. C* **34**, 1917 (1986).
- [5] J. A. Cizewski, R. F. Casten, G. J. Smith, M. L. Stelts, W. R. Kane, H. G. Börner, and W. F. Davidson, *Phys. Rev. Lett.* **40**, 167 (1978); *Nucl. Phys.* **A323**, 349 (1979)
- [6] G. Rotbard, G. Berrier, M. Vergnes, S. Fortier, J. Kalifa, J. M. Maison, L. Rosier, J. Verlotte, P. Van Isacker, and J. Jolie, *Phys. Rev. C* **47**, 1921 (1993).
- [7] J. Jolie, U. Mayerhofer, T. von Egidy, H. Hiller, J. Klora, H. Lindner, and H. Trieb, *Phys. Rev. C* **43** R16 (1991)
- [8] D. D. Warner, R. F. Casten, and A. Frank, *Phys. Lett. B* **180**, 207 (1986).
- [9] P. Van Isacker, in *Nuclear Structure, Reactions and Symmetries*, edited by R. A. Meyer and V. Paar (World Scientific, Singapore, 1986), p 231.
- [10] J. Jolie and P.E. Garrett, *Nucl. Phys.* **A596**, 234 (1996)
- [11] Zhou Chunmei, *Nucl. Data Sheets* **74**, 259 (1995).
- [12] P. D. Kunz, A DWBA computer program, University of Colorado (unpublished).
- [13] C. M. Perey and F. G. Perey, *Phys. Rev.* **132**, 755 (1963).
- [14] F. G. Perey, *Phys. Rev.* **131**, 745 (1963); Report No. ANL-6848 (unpublished), p 114.
- [15] U. Mayerhofer, T. von Egidy, G. Hlawatsch, J. Klora, and H. Lindner, *Inst. Phys. Conf. Ser. No. 88/J. Phys. G: Nucl. Phys.* **14** Suppl. S137 (1988).
- [16] U. Mayerhofer, T. von Egidy, P. Durner, G. Hlawatsch, J. Klora, H. Lindner, S. Brant, H. Seyfarth, V. Paar, V. Lopac, J. Kopecki, D. D. Warner, R. E. Chrien, and S. Pospisil, *Nucl. Phys.* **492**, 1 (1989).
- [17] D. G. Burke and G. Kajrys, *Nucl. Phys.* **A517**, 1 (1990).
- [18] M. Vergnes, G. Berrier-Ronsin, R. Bijker, *Phys. Rev. C* **28**, 360 (1983).
- [19] A. Mauthofer, K. Stelzer, Th. W. Elze, Th. Happ, J. Gerl, A. Frank, and P. Van Isacker, *Phys. Rev. C* **39**, 1111 (1989).
- [20] J. Jolie, in *Capture Gamma-Ray Spectroscopy*, edited by R. W. Hoff (IoP Publishing Ltd, Bristol, 1994), p 146.
- [21] J. Vervier, *Rivista Nuovo Cimento* **10** (1987) No 9.
- [22] A. Frank, P. Van Isacker, and D. D. Warner, *Phys. Lett. B* **197**, 474 (1987).

FIGURES

FIG. 1. Typical proton spectrum in the $^{197}\text{Au}(d,p)^{198}\text{Au}$ reaction.

FIG. 2. Typical angular distributions of protons from the $^{197}\text{Au}(d,p)^{198}\text{Au}$ reaction at 22 MeV. The curves are the result of DWBA calculations. Pure l angular distributions are shown in the upper part. An example of decomposition of a complex angular distribution is shown in the lower part: the dashed curves are the $l=1$ and 3 curves appropriately normalized. The solid curve is the sum of the two.

FIG. 3. Experimental and calculated energy spectrum of negative-parity levels in ^{198}Au . The calculated energies are obtained from (3) with parameters as given in the text. The levels are labeled by L on the left, the experimental angular momentum and parity J^- on the right, and $[N_1, N_2]$, $(\sigma_1, \sigma_2, \sigma_3)$, and (τ_1, τ_2) on top. When two values of J are possible experimentally, the chosen one is underlined.

FIG. 4. Experimental (d,p) spectrum of ^{198}Au negative parity levels up to 600 keV and comparison with present supersymmetry calculation (Calculation A) and with IBFFM calculation of ref. [16] (Calculation B). The $l=1$ spectroscopic strengths G_1 are given by the full lines lengths, the $l=3$ spectroscopic strengths G_3 by the open lines lengths. The level spin is indicated. An indication 3+1,2 means a doublet of levels, one with $J=3$, the other with $J=1$ or 2. The identifications of experimental levels with Calculation B levels are those of ref. [16]. The inconsistency that appears for the 549 keV experimental level results from an arbitrary choice of $J^\pi=0^-$ among contradictory measured spin values [11].

TABLES

TABLE I. Optical model parameters for the DWBA analysis.

	V (MeV)	r (fm)	a (fm)	W (MeV)	$4W_D$ (MeV)	r_w (fm)	a_w (fm)	r_c (fm)
d ^a	103.3	1.15	0.81	0.	78.7	1.34	0.68	1.15
p ^b	49.7	1.25	0.65	0.	40.4	1.25	0.76	1.25
n ^c	d	1.25	0.65					

^aRef. [13]

^bRef. [14]. V is adjusted with energy from 49.7 MeV for the ground state to 51.2 MeV for $E_x=2.7$ MeV.

^cA value of 25 MeV is taken for the Thomas spin-orbit form factor term of the transferred neutron.

^dAdjusted to reproduce the separation energy.

TABLE II. Experimental results for ^{198}Au below 650 keV

Ex ^a (keV)	J^π ^a	Ex ^b (keV)	G_1 ^b	G_3 ^b	$I(35^\circ)$ ^b (22MeV)	$I(35^\circ)$ ^c (20MeV)	$I(35^\circ)$ ^d (20MeV)	G_1 ^e	G_3 ^e
0.0	2 ⁻	0	0.26	0.00	100	98	100		
55.1	1 ⁻	56	0.00	0.08	12	12	11.8		
91.0	0 ⁻	(92) ^f	0.01	0.00	4	6	6.0		
192.8	1 ⁻	192	0.03	0.10	23	24	25.6		
214.8	4 ⁻	215	0.00	0.83	99	82	88		
235.9	3 ⁻	(233) ^f	} 0.15	0.00	62 ^g {	4	3.6	.01	.00
247.4	2 ⁻	245				62	68	.14	.00
259.2	1 ⁻	} 259	0.20	0.70	166 {	48	68	.20 - .00	.00 - .70
261.3	2 ⁻					82	67	.00 - .20	.70 - .00
312.0	5 ⁺	(310) ^f			5	^h	1.1		
328.3	3 ⁻	326	0.00	0.54	74	74	26		
339.3	0 ⁻	} 343	0.15	0.30	108 {	18	6.2	.04	.00
346.7	2 ⁻					80	29	.11	.30
359.4?							1.9		
362.7	2 ⁻	} 365	0.14	0.17	91 ⁱ {	24	6.7	.07 - .02	.00 - .17
368.0	1 ⁻					40	11.3	.06 - .11	.17 - .00
381.0 ^j	4 ⁻								
405.8	2 ⁻	404	0.03	0.05	19	20	7.8		
449.3	3 ⁻	} 448	0.47	0.38	242 {	200	94	.47 - .36	.02 - .38
453.6	1 ⁻ , 2 ⁻					46	19.4	.00 - .11	.36 - .00
482.1	4 ⁺ , 5 ⁺	(476) ^f			2	^h			
495.2	1 ⁻ , 2 ⁻	491			8	6	1.9		
511.2	3 ⁻	(510) ^f			3	2	1.7		
516.1?	(6 ⁺)					^h			
528.9	3 ⁻	} 528	0.05	0.00	19 {				
530.3	1 ⁻								
543.7	(4 ⁻)	} 543	0.00	0.21	30 {	16	6.4	.00	.17
548.6	1 ⁻ , 2 ⁻					4	1.8	.00	.04
570.9	1 ⁻	} 567			8 {	4	1.8		
573.3?									
625.1	3 ⁻	} 630	0.00	0.11	12 {	6	3.5	.00	.06
632.1	1 ⁻ , 2 ⁻					6	3.3	.00	.05
636.8	4 ⁺						1.4		
646.1	0 ⁺	(646) ^f			4	2	1.2		

^a From Nuclear Data Sheets [11]. Values of energy are rounded off to the nearest first decimal. A question mark "?" indicates doubt as to the existence of the level.

^b From present work. For the determination of spectroscopic strengths G , the angular distributions are assumed to correspond to a pure transfer, unless l mixing *significantly* improves the fit. The values of G_1 and G_3 correspond to respectively, a $l=1, j=3/2$ and a $l=3, j=5/2$ transfer. The relative intensities I have to be multiplied by a factor 1.75 to obtain cross-sections in $\mu\text{b}/\text{sr}$.

^c From Ref. [15]. In this paper, the relative intensities I were normalized to 100 for the largest one (level at 449 keV), giving 49 for the ground-state. Here, all values are simply multiplied by a factor 2, to obtain about 100 for the ground-state.

^d Relative intensities from Ref. [16].

^e Evaluation of spectroscopic strengths for levels not resolved in the present work. The distribution, between the members of the multiplet, of the experimental strengths (given in columns 4 and 5) determined in the present work for the unresolved "peak" is deduced (see section III) using the relative cross-sections given in columns 7 and 8.

^f This level has a small cross section and its energy is therefore not precisely determined.

^g The possible contribution of the 235.9 keV level is certainly smaller than 25% of the cross section.

^h Relative cross-sections in Ref. [15] are given only for negative parity levels.

ⁱ The possible contribution of the 381 keV level is certainly smaller than 10% of the cross section.

^j A $J^\pi = 3^+$ level is reported (Ref. [8]) at 381.5 keV, in addition to the 4^- level at 381.0 keV

TABLE III. Experimental results for ^{198}Au between 650 keV and 1.56 MeV.

Ex ^a (keV)	$J\pi$ ^a	Ex ^b (keV)	$I(35^\circ)$ ^b	G_1 ^b	G_3 ^b
663.8		669	20	0.00	0.17
672.3	3^-				
694.4	^c	695 ^d	27	^e	
696.5	(8^+)				
702.1	$(2^-, 3^-)$	704	10	0.02	0.00
703.3	$1^-, 2^-$				
728.2	^c	727	34	0.06	0.00
744.8	$1^-, 2^-$	743	14	0.00	0.07
758.0	$\geq 4^+$	763	14	0.00	0.10
764.1	$4, 5^-$				
786.1	$1^-, 2^-, 3^-$	(783) ^f	6	0.01	0.00
788.9	$1^-, 2^-$				
799.6	(3^-)	806	11	0.00	0.07
801.3	$(1^-, 2^-)$				
810.0	3^+				
811.7	(12^-)				
826.2	3^+	831	8	^e	
834.9	3^-	839	4		
868.3	3^-	(865) ^f	3		
891.1	$(2^-, 3^-)$	893 ^d	35	0.08	0.00
893.8	$2^-, 3^-$				
896.1	$1^-, 2^-$				
916.2	$1^-, 2^-$	916 ^d	19	0.03	0.04
918.1	$1^-, 2^-, 3^-$				
931.8	$(0)^-$	935 ^d	4	0.00	0.03
936.0	0^+				
952.0	3^+				
956.4	$1^-, 2^-$	960 ^d	7	0.00	0.06
961.5	$0^+, 3^+$				
971.3	3^-				
983.7	$1^+, 2^+$	(986) ^f	7		
987.0	3^-				
998.6	$1^-, 2^-$				
1018.2		^g	11		
1031.6					
1036.2					
1037.7	^{-c}				
1046.8	$1^-, 2^-$	1055 ^d	10	^e	
1056.1	2^{-h}				
1060.8					
1075.0		1071	29	0.00	0.18
1092.3	$0^-, 1^+$				

1094.9	(3) ⁺	}	1090	14	0.00	0.09 ⁱ
1105.1		}	(1106) ^f	5		
1108.9	1 ⁻ , 2 ⁻	}				
1114.7	3 ⁻	}	1121 ^d	11		
1125.5	1 ⁻ , 2 ⁻	}				
1134.8			^g	3		
1147.0	1 ⁻ , 2 ⁻	}	1156 ^d	21	0.02	0.10
1157.5	1 ⁻	}				
1160.0	3 ⁻	}				
1166.5	1 ⁻ , 2 ⁻	}	1174	24		
1175.9	1 ⁻ , 2 ⁻	}				
1191.2	1 ⁺ , 2 ⁺		(1187)	7		
1204.7	1 ⁻ , 2 ⁻	}	1205 ^d	24	0.06	0.00
1208.6	- ^c	}				
1232.7	- ^c		^g	3	0.01	0.00
1239.0	0 ⁻					
1255.8	1 ⁻ , 2 ⁻	}				
1266.0	- ^c	}	1269	11	0.00	0.08
1272.0	3 ⁻	}				
1286.1	0 ⁻ , 3 ⁻					
1292.4	1 ⁻ , 2 ⁻					
1296.8		}	1301	22	^e	
1301.5	1 ⁻ , 2 ⁻	}				
1305.7		}				
1307.3	3 ⁻					
1318.3	1 ⁻ , 2 ⁻	}	(1320) ^d	8	0.02	0.00
1326.1	- ^c	}				
1334.8	3 ⁻	}	(1339) ^f	6	0.00	0.04
1338.3	3 ⁻	}				
1359.4	-	}	^g	3		
1363.9	3 ⁻	}				
1371.3	1 ⁻ , 2 ⁻	}	1379 ^d	14	0.00	0.07
1376.7	1 ⁻ , 2 ⁻	}				
1380.9	0 ⁻ , 3 ⁻	}				
1390.0	0 ⁻	}	^g	5		
1395.8	3 ⁻	}				
1399.8						
1403.4	1 ⁻ , 2 ⁻ , 3 ⁻	}	1405 ^d	14	0.00	0.08
1405.9	1 ⁻ , 2 ⁻ , 3 ⁻	}				
1409.5	0 ⁻ , 3 ⁻	}				
1417.6	3 ⁺					
1424.5	- ^c	}	1435	11		
1431.6	- ^c	}				
1435.2	- ^j	}				

1443.6	- ^c					
1452.7	- ^c					
1459.4	3 ⁻	}	g	15		
1471.7	3 ⁻					
1476.0	1 ⁻ , 2 ⁻	}	1485	37		
1487.4						
1496.7	3 ⁻					
1505.4	1 ⁻ , 2 ⁻	1509	}	24	0.00	0.13
1513.6	1 ⁻	1517				
1523.2	1 ⁺ , 2 ⁺ , 3 ⁺					
1530.1	1 ⁻ , 2 ⁻					
1536.4	- ^c					
1542.1	3 ⁻	}	g	26	0.03	0.07
1553.8	1 ⁻ , 2 ⁻					
1560.0	3 ⁻					

^a From Nuclear Data Sheets [11]. Values of energy are rounded off to the nearest first decimal.

^b From present work. For the determination of spectroscopic strengths G, the angular distributions are assumed to correspond to a pure transfer, unless *l* mixing *significantly* improves the fit. The values of G_1 and G_3 correspond to respectively, a $l=1, j=3/2$ and a $l=3, j=5/2$ transfer. The relative intensities *I* have to be multiplied by a factor 1.75 to obtain cross-sections in $\mu b/sr$.

^c No *J* value is given in the Adopted Levels Table of Nuclear Data Sheets when assignments from different methods are not consistent.

^d Probable unresolved multiplet.

^e Angular distribution consistent with a $l = 4$ transfer. The corresponding $g_{9/2}$ spectroscopic strengths are 0.13 for the 695 keV peak, 0.05 for the 831 keV peak, 0.07 for the 1055 keV peak, and 0.12 for the 1301 keV peak.

^f This level has a small cross section and its energy is therefore badly determined.

^g No peak is observed. The strength given in the next column corresponds to the energy region indicated by the bracket.

^h The value $J^\pi = 12^-$ in Nuclear Data Sheets is clearly a misprint.

ⁱ *l* value not consistent with the J^π assignment in column 2.

^j Doublet with J^π probably 0^- to 3^- for both components.

TABLE IV. Main experimental results above 1560 keV

Ex/keV	$I(35^\circ)$	G_1	G_3
2224 ^a	32	0.00	0.15
2245 ^a	74	0.00	0.30
2266	} 117	0.00	0.49
2283			
2296	} 70	b	
2304 ^a			
2326 ^a	33	0.00	0.16
2343	21	0.05	0.00
(2361)	15	0.00	0.07
2381	26	b	
2393	20	c	
2469 ^a	48	c	
2479	54	0.00	0.19
2490	43	0.00	0.18
2505	33	0.00	0.11
(2520) ^a	18	0.00	0.08
2598 ^a	(16) ^d	0.00	0.06
2610 ^a	(30) ^d	0.00	0.12

^aProbable unresolved multiplet.

^bAngular distribution consistent with a $l=4$ transfer. The corresponding $g_{9/2}$ spectroscopic strengths are 0.32 for the 2296+2304 keV peak, 0.11 for the 2381 keV peak.

^cThe angular distribution is consistent with a $l=5$ transfer with a $h_{9/2}$ spectroscopic strength of 0.60 for the 2393 keV peak, with a $l=6$ transfer with $G_{13/2}=1.18$ for the 2469 keV peak.

^dPeak hidden at 35° by the ground state peak of the (d,p) reaction on ^{12}C . The average of cross sections at 30° and 40° is given within parenthesis.

 TABLE V. Summed $l=1$ and $l=3$ experimental strengths for pick-up reactions on the N=118 targets ^{197}Au and ^{196}Pt (from Ref. [6]: see text).

	$\sum C^2S$	^{197}Au	^{196}Pt
$l=1$	a	3.28	3.41
	b	2.49	2.56
	c	2.25	2.56
$l=3$	a	6.23	6.59
	b	2.06	3.89
	c	2.01	3.89

^aTotal observed strength up to 1.2 MeV in ^{195}Pt , up to 1.5 MeV in ^{196}Au .

^bStrength observed up to 600 keV for all the levels.

^cStrength observed up to 600 keV, excluding levels with $C^2S < 0.1$.

TABLE VI. Summed $l=1$ and $l=3$ experimental strengths for stripping reactions on the $N=118$ targets ^{197}Au and ^{196}Pt (from present work and Ref. [17]: see text).

	ΣG	^{197}Au	^{196}Pt
$l=1$	a	2.0	
	b	1.83	1.80
	c	1.49	1.59
	d	1.37	1.54
$l=3$	a	7.5	
	b	4.85	4.68
	c	3.36	2.42
	d	3.31	2.42

^aTotal observed strength up to 2.7 MeV for ^{198}Au .

^bTotal observed strength up to 1.56 MeV for ^{198}Au , up to 1.82 MeV for ^{197}Pt .

^cStrength observed up to 600 keV for all the levels.

^dStrength observed up to 600 keV, excluding levels with $G < 0.08$.

TABLE VII. Classification of $1/2^-$, $3/2^-$, and $5/2^-$ states, and values of the strengths in the $^{196}\text{Pt} \rightarrow ^{197}\text{Pt}$ reaction.

J^π	Ex/keV	Classification	G_{expt}	G_{calc}
$1/2^-$	0	$[[6, 0](6, 0, 0)(0, 0)0 1/2]$	0.38	0.38
$5/2^-$	53	$[[5, 1](5, 1, 0)(1, 0)2 5/2]$	1.72	1.72
$3/2^-$	72	$[[5, 1](5, 1, 0)(1, 0)2 3/2]$	0.34	0.34
$3/2^-$	99	$[[5, 1](5, 1, 0)(1, 1)1 3/2]$	0.59	0.59
$1/2^-$	131	$[[5, 1](5, 1, 0)(1, 1)1 1/2]$	0.23	0.23
—	—	$[[5, 1](5, 1, 0)(1, 1)3 5/2]$	~ 0	0.00
$3/2^-(1/2)^-$	269	$[[6, 0](6, 0, 0)(1, 0)2 3/2]$	0.01	0.01
$5/2^-$	299	$[[6, 0](6, 0, 0)(1, 0)2 5/2]$	0.08	0.08
$1/2^-, 3/2^-$	426	$[[5, 1](5, 1, 0)(2, 0)2 3/2]$	~ 0	0.14
$5/2^-$	457	$[[5, 1](5, 1, 0)(2, 0)2 5/2]$	0.08	0.08
$3/2^-$	502	$[[5, 1](5, 1, 0)(2, 1)1 3/2]$	0.04	0
$3/2^-$	708	$[[6, 0](6, 0, 0)(2, 0)2 3/2]$	0.09	0.09
—	—	$[[6, 0](6, 0, 0)(2, 0)2 5/2]$	~ 0	0.05
$1/2^-$	748	$[[5, 1](4, 0, 0)(0, 0)0 1/2]$	0.04	0.04

TABLE VIII. Experimental and calculated energies (in keV) and strengths for the lowest negative-parity levels of ^{198}Au populated by neutron stripping.

E_x^a	J^π ^a	G_1^b	G_3^b	E_x^c	J^π ^c	G_1^c	G_3^c
0	2^-	0.26	0.00	0	2_1^-	0.26	0.00
55	1^-	0.00	0.08	104	1_1^-	0.04	0.10
91	0^-	0.01	0.00	164	0_1^-	0.05	-
193	1^-	0.03	0.10	120	1_2^-	0.12	0.00
215	4^-	0.00	0.83	269	4_1^-	-	0.51
236	3^-	0.01	0.00	280	3_2^-	0.02	0.08
247	2^-	0.14	0.00	304	2_3^-	0.02	0.28
259	1^-	}0.20	0.70{	204	1_3^-	0.003	0.002
261	2^-			260	2_2^-	0.02	0.00
328	3^-	0.00	0.54	180	3_1^-	0.22	0.55
339	0^-	0.04	0.00	264	0_2^-	0.00	-
347	2^-	0.11	0.30	360	2_4^-	0.12	0.07
363	2^-	}0.13	0.17{	440	2_5^-	0.00	0.01
368	1^-			380	1_4^-	0.03	0.00
381	4^-	0.00	0.00	369	4_2^-	-	0.04
406	2^-	0.03	0.05	460	2_6^-	0.01	0.01
449	3^-	}0.47	0.38{	315	3_3^-	0.11	0.00
454	$1^-, 2^-$			424	1_5^-	0.08	0.04
495	$1^-, 2^-$	0.00	0.00	495	2_7^-	0.05	0.00
511	3^-	0.00	0.00	509	3_5^-	0.08	0.03
529	3^-	}0.05	0.00{	495	3_4^-	0.002	0.01
530	1^-			508	1_6^-	0.01	0.002
544	$(4)^-$	0.00	0.17	584	4_3^-	-	0.02
549	$1^-, 2^-$	0.00	0.04	540	2_8^-	0.00	0.01
571	1^-	0.00	0.00	554	1_7^-	0.00	0.00

^aFrom Nuclear Data Sheets. Values of energy are rounded off to the nearest integer value.

^bExperimental values from present work. (see Table II)

^cCalculated values from present work. (see Section V.A)

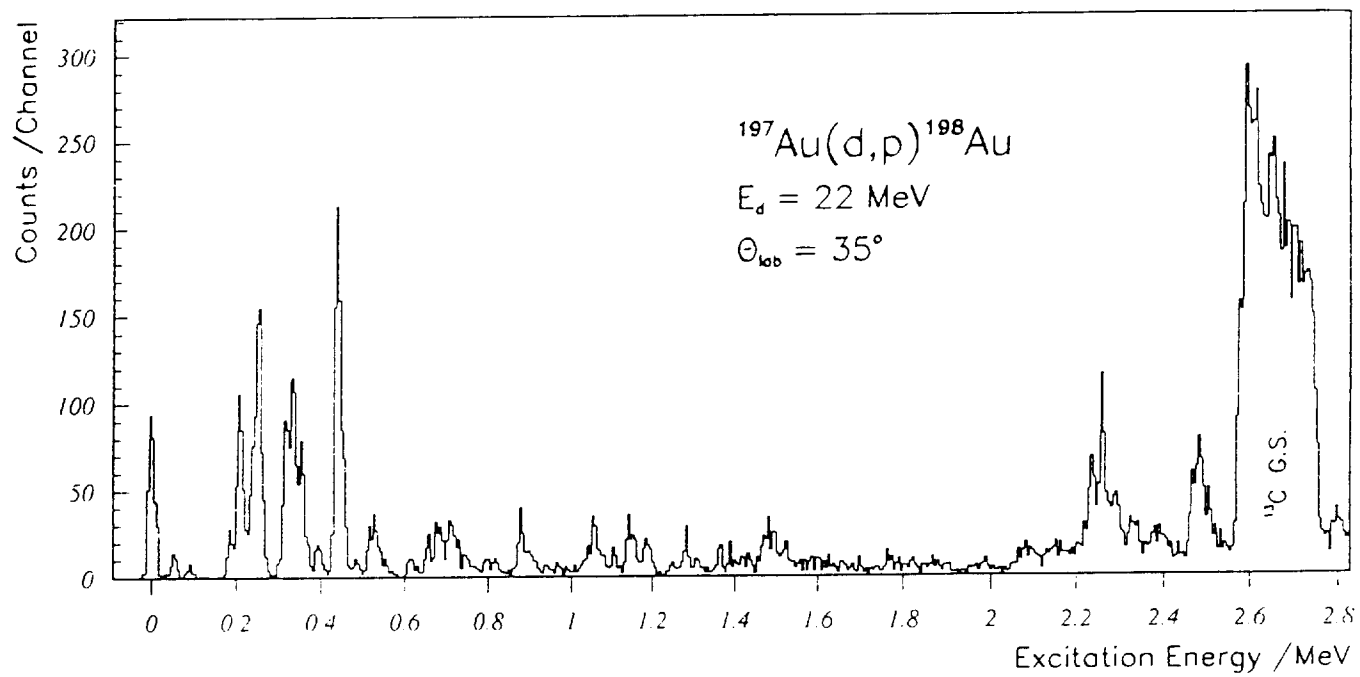


Fig. 1



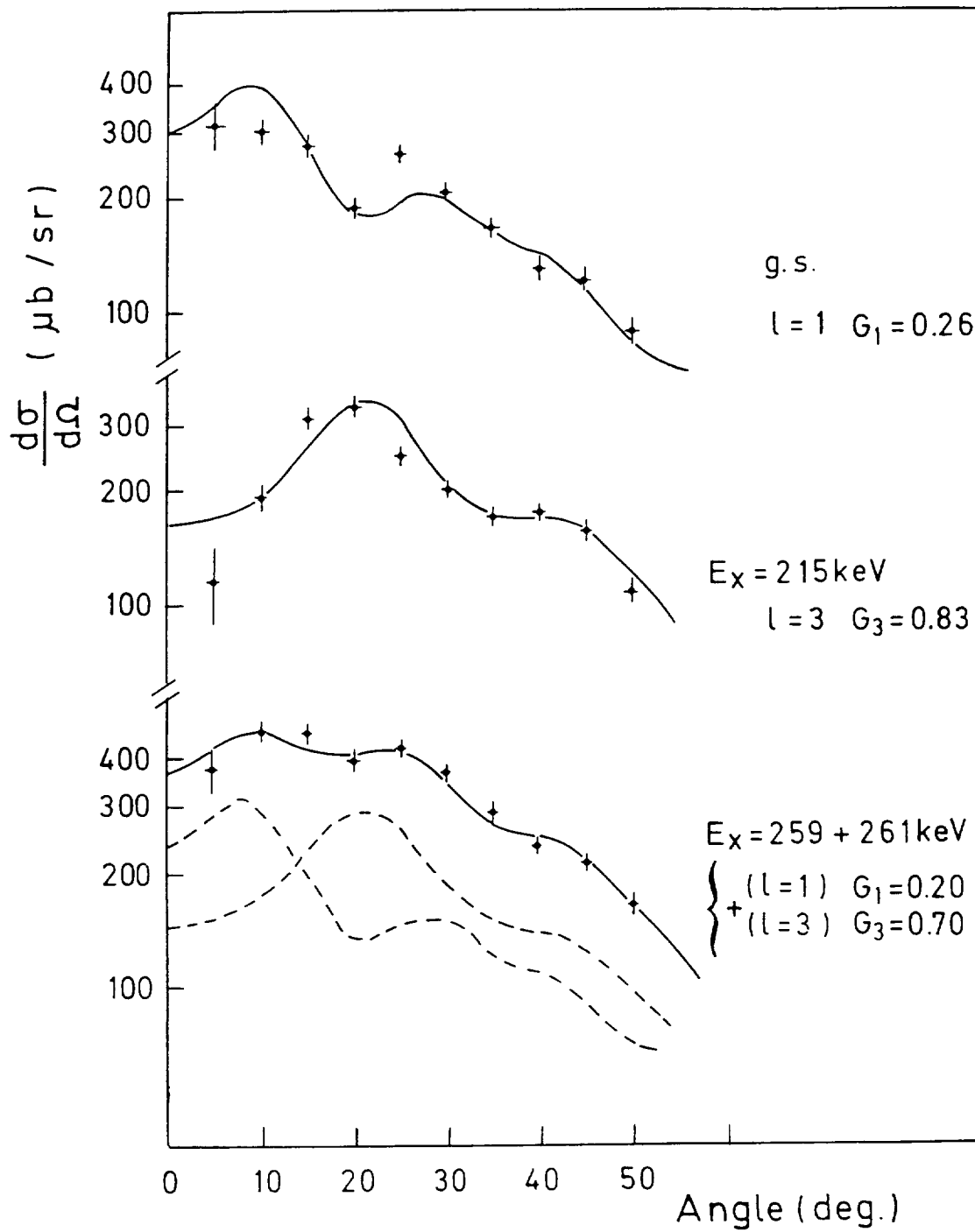


Fig. 2



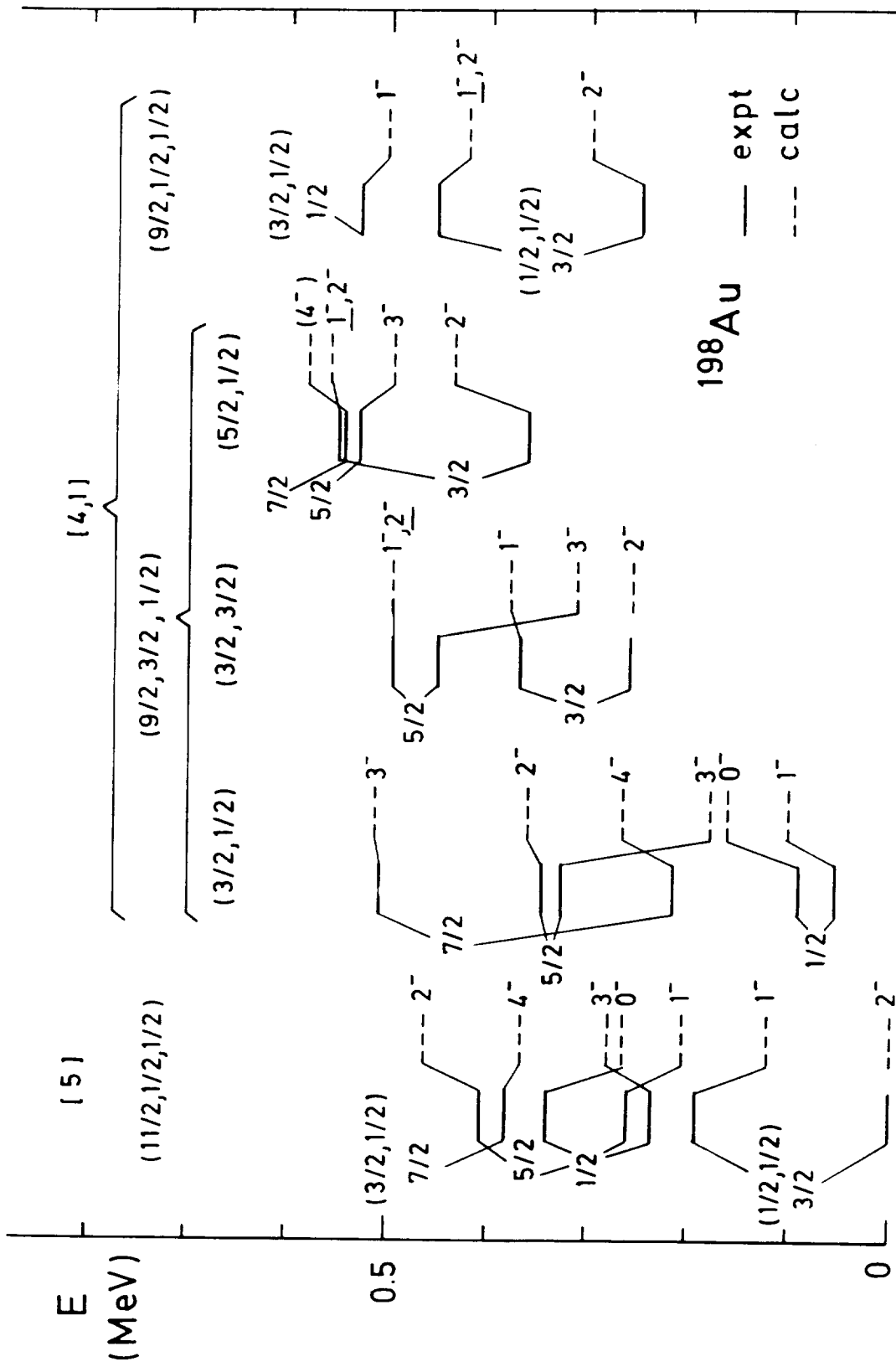


Fig. 3



198Au

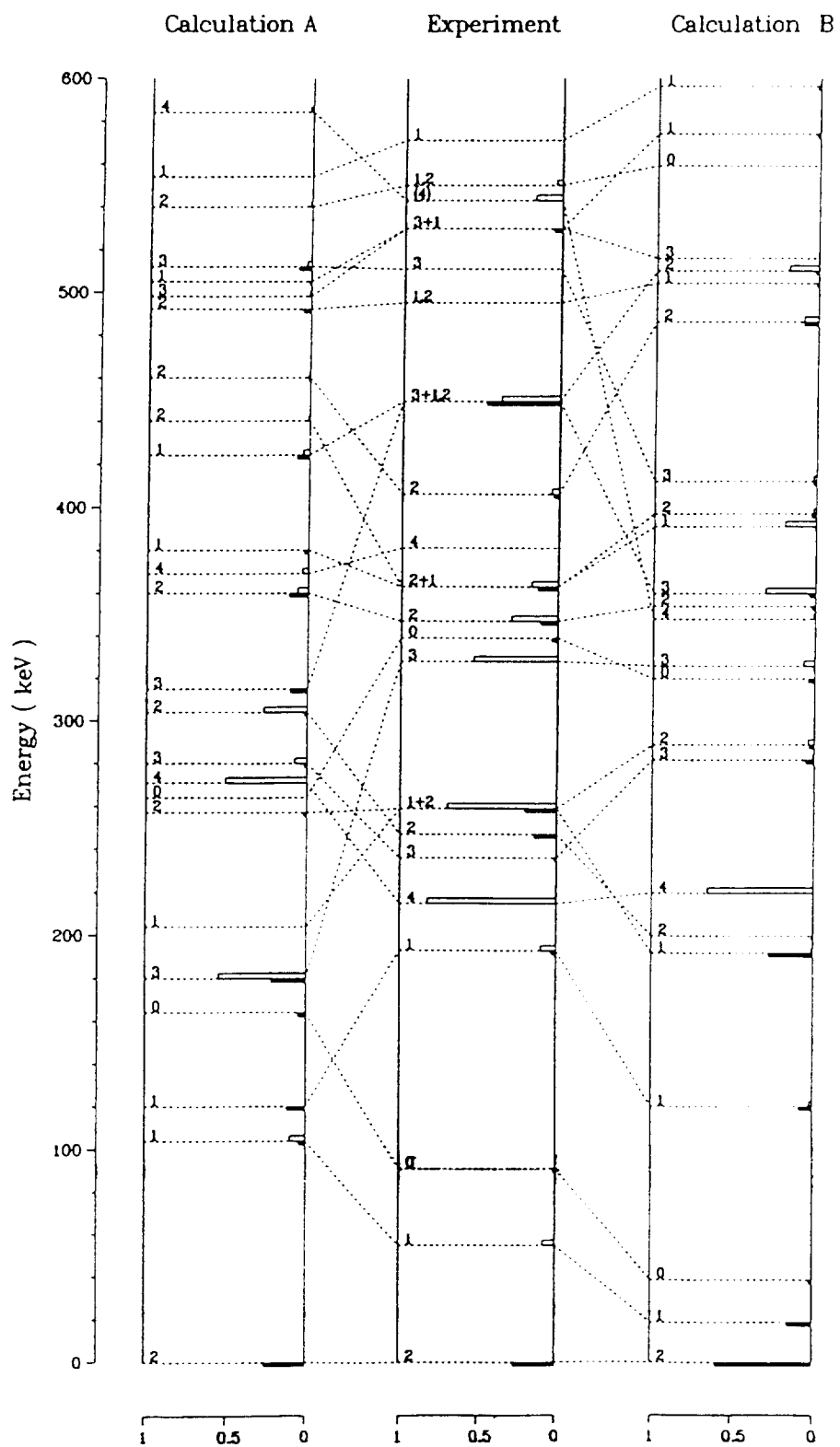


Fig. 4

